Journal of Power and Energy Systems

Vol. 4, No. 2, 2010

Power Generation Efficiency of Photovoltaics and a SOFC-PEFC Combined Micro-grid with Time Shift Utilization of the SOFC Exhaust Heat*

Abeer Galal El-Sayed** and Shin'ya OBARA***

**Kitami Institute of Technology,

165 Koen-cho, Kitami, Hokkaido 090-8507, Japan

***Department of Electrical and Electronic Engineering, Kitami Institute of Technology,

E-mail: obara@indigo.plala.or.jp

Abstract

In this study, the combined system of a solid-oxide fuel cell (SOFC) and a proton-exchange membrane fuel cell (PEFC) is developed. The proposed system consists of a SOFC-PEFC combined system and a photovoltaic system (PV) as the energy supply to a micro-grid. The exhaust heat of the SOFC is used for the steam reforming of the bio-ethanol gas with time shift utilization of the exhaust heat of the SOFC in optional time. The SOFC-PEFC combined system with the PV was introduced in a micro-grid of 30 residences in Sapporo, Japan. The operation plan of the system has three cases: without solar power, with 50% and with 100% of solar output power. Moreover, three types of system operation of using the SOFC independent operation, PEFC independent operation and SOFC-PEFC combined system are used to supply the demand side. A comparative study between the types of system operation is presented. The power generation efficiency is investigated for different load patterns: average load pattern, compressed load pattern and extended load pattern. This paper reported that the power generation efficiencies of the proposedsystem in consideration of these load patterns are 27% to 48%.

Key words: Fuel Cell, Micro-Gird, Combined System, SOFC, PEFC, Photovoltaics, Operation Planning

1. Introduction

The solid-oxide fuel cell (SOFC) is recognized as the most efficient fuel cell among various fuel cells. The SOFC is considered an energy conversion device due to its several potential benefits, including low pollutant emissions, high-energy efficiency, the possibility of using different kinds of fuels and the possibility of building hybrid systems [1-3]. As a fuel cell for residences, proton-exchange membrane fuel cell (PEFC) and SOFC were developed. Though higher temperatures are required with SOFC in comparison with PEFC, the power generation efficiency is high and the uses for exhaust heat are wide. In order to utilize the hot exhaust heat of SOFC effectively, the SOFC and gas turbine (GT) compound system was developed [4-8]. Although high thermal efficiency is achieved in the SOFC-GT compound system, maintenance of the high thermal efficiency is difficult. Moreover, because the partial load quality of GT is bad, it is difficult to maintain the power generation

*Received 2 Nov., 2009 (No. 09-0670)
[DOI: 10.1299/jpes.4.274]

efficiency of the whole system. In this system, it is necessary to perform synchronous operation the exhaust heat output from the SOFC and the driving of GT. Consideration of the load characteristic of the demand side is indispensable to investigate the power generation efficiency. Moreover, an operation plan with high power generation efficiency by a high load factor is required.

In this paper, the exhaust heat of SOFC is used for the steam reforming of bio-ethanol fuel. The reformed gas is stored in a cylinder; this reformed gas is supplied to the PEFC when needed. In other words, time shift utilization of the exhaust heat of the SOFC is installed. When using this time shift utilization of the exhaust heat of the SOFC, the operation of the system can be planned so that a load peak is cut. In addition, in this study, the SOFC-PEFC and PV combined system are proposed to supply power and heat to 30 residences in Sapporo, Japan. The SOFC of the proposal system is made to correspond to a base load, and the PEFC is made to correspond to fluctuating load. The exhaust heat of the SOFC supplies the steam reformer and makes reformed gas. This reformed gas is stored and used for the operation of the PEFC the following day.

In this study, the optimized operation of a micro-grid with the SOFC-PEFC and PV combined system at different load patterns is clarified. A comparative study is performed between SOFC-independent operation, PEFC-independent operation and SOFC-PEFC combined system operation. The optimization analysis of the operation plan considers the operation of a power system and a heat system. Moreover, the power generation efficiency and the operation planning of the boiler are investigated.

2. System configuration

2.1 System scheme

The proposed micro-grid with a SOFC-PEFC and PV combined system is shown in Fig. 1. A schematic figure of the proposed system is shown in Fig. 1(a). It consists of the SOFC-PEFC combined system, PV system, power conditioning system, heat supply system and system controller. The details of each system are shown in Figs. 1(b) to (e). Each piece of equipment of the proposal system is operated by the system controller [9]. The electric power and heat of the SOFC-PEFC combined system and PV system are used to supply power and heat to a grid of 30 residences in Sapporo in Japan. The electricity production for every sample time for each day is predicted by using NWI (the numerical weather information) [10, 11] obtained by the system controller, as shown in Fig. 1(a). The exhaust heat outputted from the SOFC is hot, at 750 ℃ - 900 ℃ . This high temperature exhaust heat is used for the steam reforming of bioethanol and the heating of LNG (liquid natural gas) and air supplied to the SOFC. The reformed gas is stored in a cylinder. The power load peak of the following day is cut by supplying the stored reformed gas to the PEFC. Such system management is planned by the system controller. The SOFC-PEFC combined system is examined by using the different electrical load patterns of the micro-grid.

2.2 SOFC and PEFC combined system

(a) Power grid

The block diagram of the SOFC-PEFC combined system used in the proposal system is shown in Fig. 1(b). The SOFC that is introduced into the system has an internal reformer. As shown in this figure, the exhaust heat of SOFC heats the LNG, bio-ethanol gas and the air, which are supplied to the SOFC cathode using the heat exchanger (HEX). Supplying the exhaust heat of the SOFC to the steam reformer (R/M) with a shift unit (S/U) produces a reformed gas with a high hydrogen density [12-14]. Moisture is present in the reformed gas, so

a condenser unit (C/U) for air cooling is used. A CO oxidation device (C/O) is used to remove CO from the reformed gas. After decreasing the CO content, the reforming gas is stored in the cylinder by a compressor (C/P). The electric power of the SOFC and PEFC is supplied to the DC-DC and the DC-AC converter and inverter, then to the power grid [15— 17].

(b) Heat grid

The exhaust heat of the SOFC with an internal reformer is used for heating the LNG, bio-ethanol gas and the air supplied to the SOFC cathode. The remaining exhaust heat is supplied to the steam reformer (R/M). The exhaust heat of the reforming unit, condenser unit (C/U) and PEFC is stored in the heat storage tank. The heat exchanger is installed in the heat storage tank. Heat is exchanged between the tap water and the heat medium in the heat storage tank [15— 17]. A boiler is operated when there is little heat storage compared with the heat demand.

2.3 Photovoltaic (PV) system

The block diagram of the PV system is shown in Fig. 1(e). As shown in the figure, the proposed PV system consists of a solar cell, DC-DC converter and DC-AC converter. The

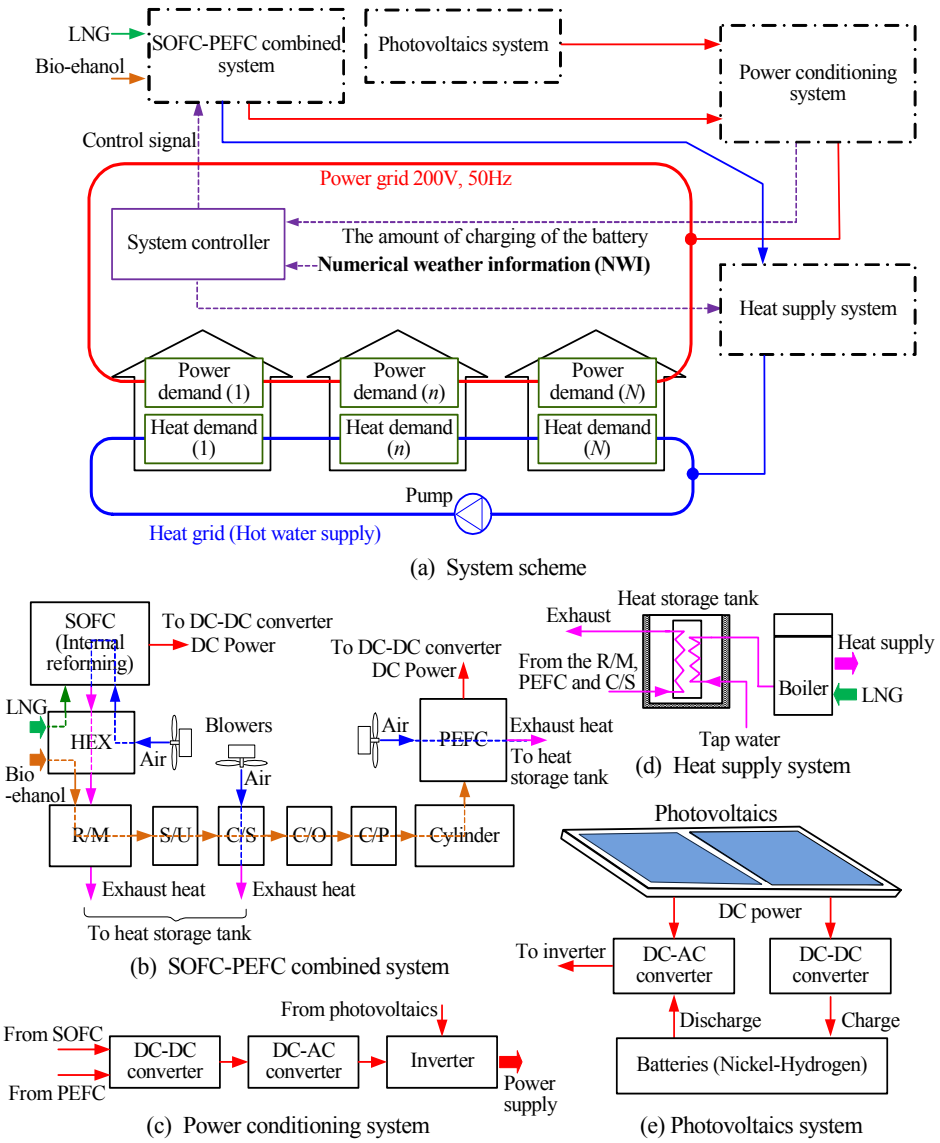

C/O : CO oxidation unit, C/S : Condenser unit, HEX : Heat exchanger, R/M : Reformer, S/U : Shift unit

Fig. 1 Proposal microgrid with photovoltaics and SOFC-PEFC combined power system

power output from the solar cell can be supplied to the power demand through an inverter. The type of solar cell used is a polycrystalline silicon solar module. The following equations are used to calculate the electricity production $P_{s,t}$ from the solar module [18-20].

$$P_{s,t} = S_S \cdot \eta_S \cdot (H_{D,t} + H_{S,t}) \cdot \{1 - (T_{C,t} - T_O) \cdot (R_T / 100)\} \quad (1)$$

where $P_{s,t}$ is the output power from the solar cell, $H_{D,t}$ is the direct solar radiation intensity, $H_{S,t}$ is the sky solar radiation intensity, $T_{C,t}$ is the temperature of the solar cell, S_S is the area of the solar cell (72 m^2), η_S is the generation efficiency (14%), R_T is the temperature coefficient (0.4%/K), and T_O is the reference temperature (298K). Direct solar radiation and sky solar radiation are used for power generation in a flat solar cell. The global-solar-radiation intensity ($I_{H,t}$), horizontal sky solar radiation intensity ($I_{S,t}$) and direct solar radiation intensity ($I_{D,t}$) at time t (t=0, 1, 2, 3,.....,23) can be determined from the NWI [18, 19].

$$H_{D,t} = I_{D,t} \cdot \cos\theta \quad (2)$$

$$\sin\theta = \cos\alpha \cdot \sin\delta - \sin\alpha \cdot \cos\varphi \cdot \cos\delta \quad (3)$$

$$H_{S,t} = 0.5 \cdot I_{S,t} \cdot (1 + \cos\beta) + 0.5 \cdot \lambda \cdot I_{H,t} \cdot (1 - \cos\beta) \quad (4)$$

$$\cos\beta = \cos\alpha \cdot \cot\varphi + \sin\alpha \cdot \mathrm{cosec}\varphi \cdot \tan\delta \quad (5)$$

where λ is the reflection factor, θ is the incident angle to the acceptance surface of the sunlight, α is the latitude of the setting point, δ is the solar celestial declination, φ is the hour angle, and β is the angle of the gradient of the acceptance surface.

2.4 Operation of the SOFC-PEFC combined system

Figure 2 (a) shows the power division rate of the SOFC-PEFC combined system that is introduced to the demand side. As shown in this figure, the operation plan of the SOFC corresponds to the base load. On the other hand, the operation plan of the PEFC is in accordance to the load fluctuation. The base load is set as a larger value than the minimum

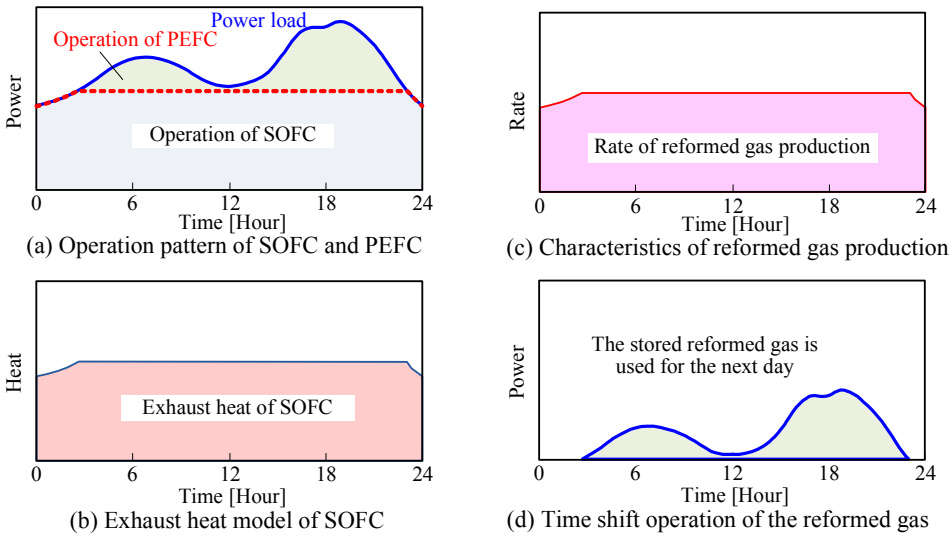

(a) Operation pattern of SOFC and PEFC
(c) Characteristics of reformed gas production
(b) Exhaust heat model of SOFC
(d) Time shift operation of the reformed gas

Fig. 2 Power division rate of the SOFC-PEFC combined system

value of the load fluctuation, so the SOFC is operated with maximum generation efficiency. The amount of exhaust heat from the SOFC-PEFC combined system depends on the operation plan of the SOFC, as shown in Fig. 2(b). In addition, the quantity of reformed gas produced changes with the setting of the load of the SOFC, as shown in Fig. 2(c). In Fig. 2(d), the stored reformed gas is supplied to the PEFC, and it is used the next day.

Equations from (6) to (12) show the steam reformation of bio-ethanol gas and the hydrogen production process, as described before. Here, (l) and (g) show the state of the liquid and gas, respectively.

$$H_2O(l) \rightarrow H_2O(l) - 0.1924\text{kJ/(mol}\cdot\text{K)} \tag{6}$$

$$C_2H_5OH(l) \rightarrow C_2H_5OH(l) - 0.113\text{kJ/(mol}\cdot\text{K)} \tag{7}$$

$$H_2O(l) \rightarrow H_2O(g) - 40.6\text{kJ/mol} \tag{8}$$

$$C_2H_5OH(l) \rightarrow C_2H_5OH(g) - 38.6\text{kJ/mol} \tag{9}$$

$$C_2H_5OH + 3H_2O \rightarrow 2CO_2 + 6H_2 - 173\text{kJ/mol} \tag{10}$$

$$C_2H_5OH + 3O_2 \rightarrow 2CO_2 + 3H_2O + 1369\text{kJ/mol} \tag{11}$$

$$H_2 + 1/2O_2 \rightarrow 3H_2O + 287\text{kJ/mol} \tag{12}$$

2.5 Partial load quality

Figure 3(a) shows the power generation efficiency of the SOFC at different load factors [20, 21] for the SOFC accompanied by internal reforming. Figure 3 (b) is the efficiency of the PEFC at different load factors, where the PEFC is accompanied by a steam reformer related to the power generation efficiency [22, 23]. When comparing Figs 3 (a) and 3 (b), the power generation efficiency of the SOFC at a load factor of 25% or more is high in comparison with the PEFC. In addition, at a load factor less than 25%, the power generation efficiency of the SOFC decreases greatly. Therefore, a SOFC load factor of 25% or less is usually not advisable. Moreover, the reformer efficiency η_R in Fig. 3 (b) is defined by the following equation:

$$\eta_R = \frac{\text{Heating value of reformed gas}}{\text{Heating value of supply bioethanol}} \tag{13}$$

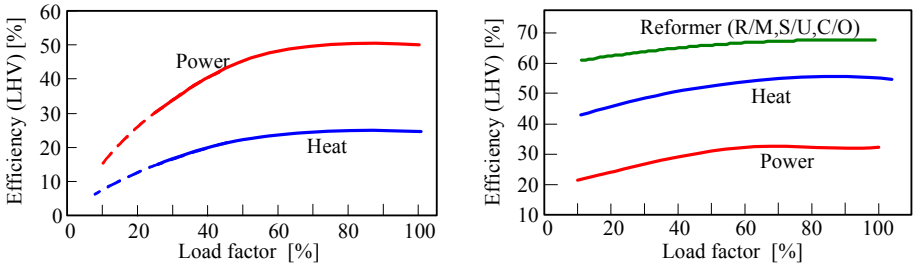

(a) SOFC with internal reforming (b) PEFC with steam reformer

Fig. 3 Power generation efficiency of SOFC and PEFC, and reformer efficiency

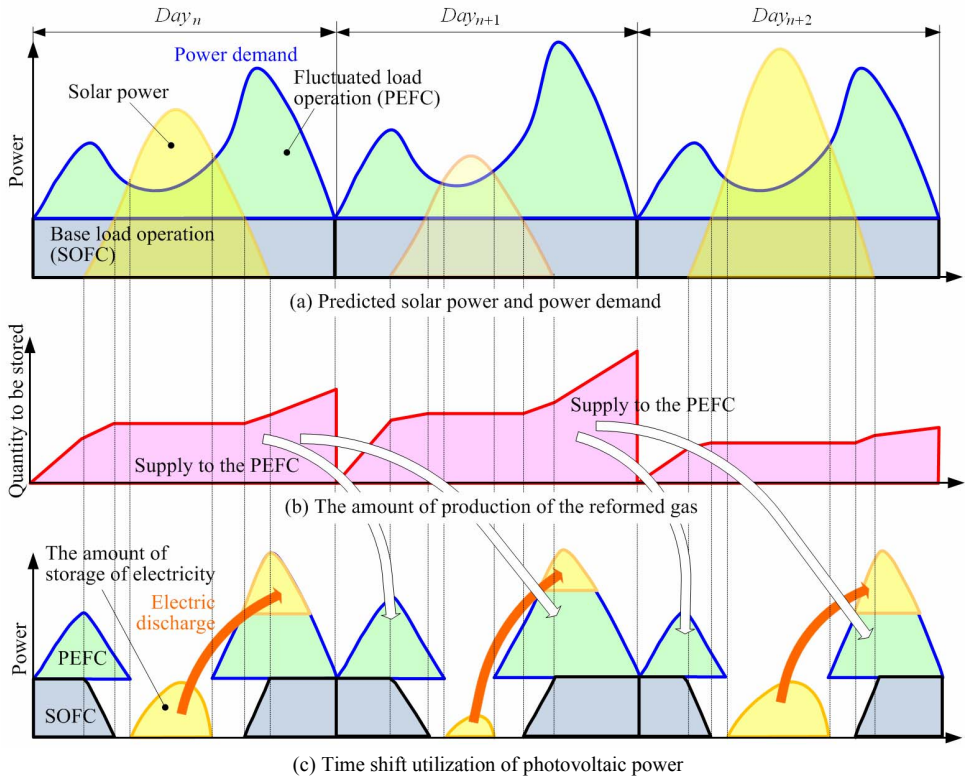

Fig. 4 Power operation method of the proposal microgrid

2.6 Operation plan of the proposal system

Figure 4 shows the power operation method of the proposal system for three days (Day_n , Day_{n+1} and Day_{n+2}). The predicted output power from the solar cell and the power demand are shown in Fig. 4 (a). In this figure, the operation plan of the SOFC and PEFC are shown. Moreover, the base load of the SOFC is shown. Figure 4 (b) shows the amount of production of reformed gas each day. After storing this reformed gas, it is supplied to the PEFC to use the following day. Figure 4 (c) shows the operation of the PEFC using the reformed gas produced on the previous day.

3. Demand pattern

Figures 5 (a) and (b) are the compressed model of the width of daily power load fluctuations (compressed load pattern) and the extended model of the width of daily load fluctuations (extended load pattern), respectively. These patterns compress and extend fluctuations of the average load of power demand on a representative day to 50% and 150%, respectively. Here the load integration value (the amount of power demand on the representative day) of both patterns is the same as the total power demand under an average load. As a result, this paper investigates the electricity demand model of the microgrid of the three patterns, as shown in Fig. 6. This figure is an example of a representative day in February of 30 residences in Sapporo [24, 25]. The electricity demand includes appliances and electric lighting. The thermal demand comes from heating, hot water supply and baths. In the SOFC-PEFC combined system, the production quantity of reformed gas depends on the operation method of the SOFC, so the electric power demand pattern of the micro-grid affects the operation plan of the proposal system. In the analysis, three load patterns, the average load pattern, the extended load pattern and the compressed load pattern, are investigated.

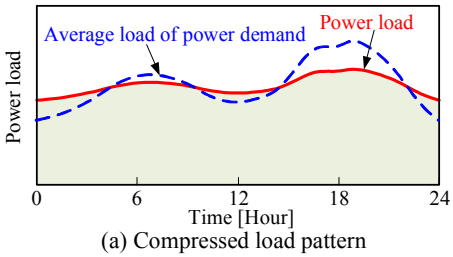

(a) Compressed load pattern

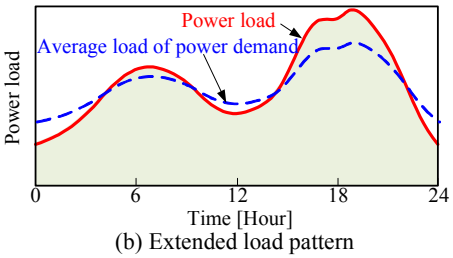

(b) Extended load pattern

Fig. 5 Power demand model of the microgrid

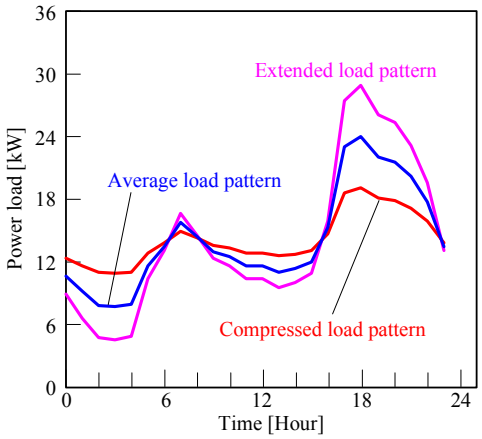

Fig. 6 Power demand pattern of the microgrid (Sapporo in Japan, 30 houses, February representative day)

4. Analysis method

The analysis procedure of the SOFC-PEFC combined system is described as follows.

(1) First, the predictive values of the power load pattern (Fig. 6) and the production of electricity of the photovoltaic power (Fig. 4 (a)) are obtained for every sampling time. However, such an analysis method of power load estimation and output prediction of photovoltaic power should be considered separately. On the other hand, the production of the electricity of the photovoltaic power is predicted using the NWI described by Section 2.1. The amount of solar radiation and the outside air temperature for every sampling time can be obtained by the NWI. Moreover, the output of photovoltaic power can be obtained by introducing the installation angles of the solar cell to Eqs. (1) to (5).

(2) The boundary value (i.e., capacity of the SOFC) between the base load and the load following is decided using the power demand pattern obtained by (1) (Fig. 2 (a)). Here, this boundary value is decided using the power demand pattern of a representative day with the highest peak of the power load. In this study, the extended power load pattern of a

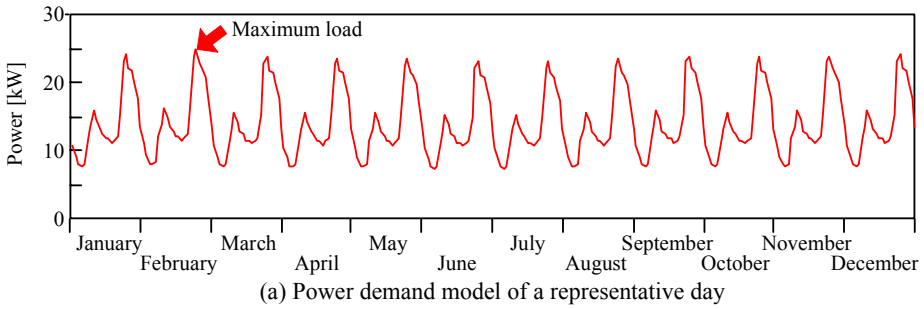

(a) Power demand model of a representative day

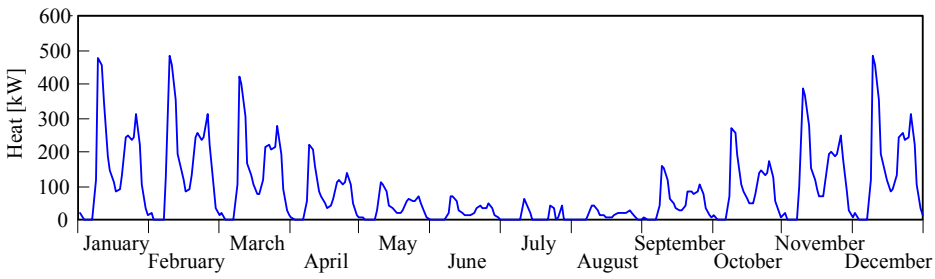

(b) Heat demand model of a representative day

Fig. 7 Energy demand pattern of the microgrid. Sapporo-city in Japan, 30 houses.

representative day in February is used.

(3) The amount of power demand and the production of electricity from photovoltaic power generation are compared for each sampling time. When there is a greater amount of photovoltaic power than power demand, the surplus power is charged to a battery. On the other hand, the storage power is discharged during the load peak in the evening.

(4) The SOFC operates as shown in Figs. 2 (a) to (c). On the other hand, the PEFC is operated to respond to the fluctuating power load. The reformed gas produced by the exhaust heat of the SOFC on the previous day is used for the PEFC operation.

(5) The amount of exhaust heat of the SOFC is obtained from Fig. 3 (a) for every sampling time. The amount of reformed gas (namely, the amount of hydrogen) outputted from the C/O in Fig. 1 (b) is obtained from the amount of SOFC exhaust heat using Eqs. (6) to (12). The reformed gas is stored in a cylinder and is used in the operation of the PEFC the next day. As described in (2), the boundary value between the base load zone and the factual load zone is decided using the power load pattern of a representative day with the highest power load peak. Therefore, a shortage of the storage reformed gas used for the operation of the PEFC the following day is not assumed.

(6) The amount of exhaust heat from the R/M, C/U and PEFC shown in Fig. 1 (b) is

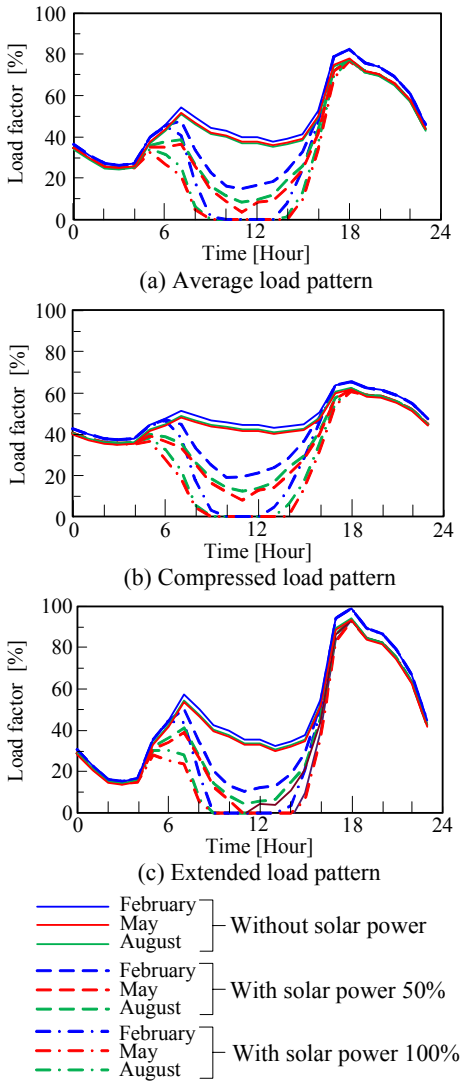

Fig. 8 Load factor of the SOFC and PEFF without storage of electricity

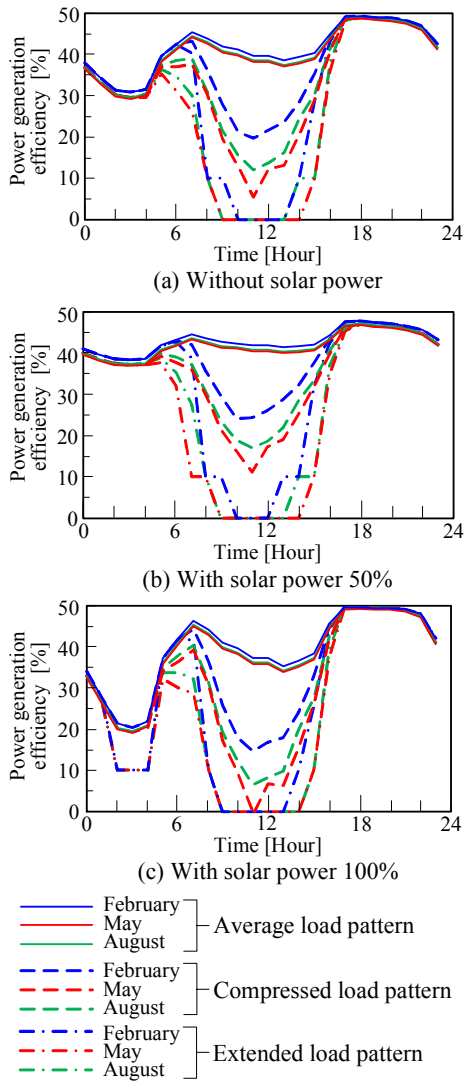

Fig. 9 Power generation efficiency of the SOFC

obtained from the heat balance. This exhaust heat is stored in a heat storage tank. Heat storage losses are 0.5%/hour supposing a real system. The balance of heat is calculated for every sampling time. When the amounts of heat storage run short of the heat demanded, a boiler with 90% efficiency is operated.

(7) The fuel consumption (which is expressed with the heating value) of the SOFC is calculated in the case of the operation of the proposal system according to (1) to (6), R/M and a boiler. By the operation of the proposed system based on (1) to (6), the fuel consumption of the SOFC, R/M and the boiler is calculated. The rate of the power supply of the SOFC and PEFC to the heating value of the fuel supplied to the SOFC and R/M is defined as the power generation efficiency.

5. Results and discussion

The maximum electrical load of the micro-grid appears in February, as shown in Fig. 7(a). Therefore, the capacity of the SOFC or PEFC will be decided with the extended load pattern in a representative day in February. Thus, the capacity (30 kW) is decided for the operation analysis with the independent operation of the SOFC and PEFC. In the SOFC-PEFC combined system, the total capacity of the SOFC and PEFC is 30 kW. In addition, the capacities of the SOFC and PEFC are 25.5 kW and 4.5 kW respectively.

Figure 8 shows the load factor of the SOFC and PEFC at different load patterns

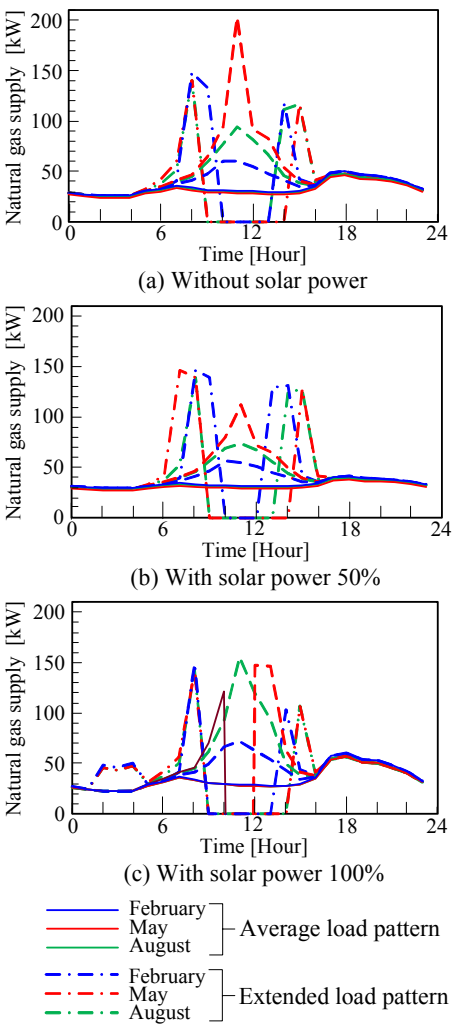

Fig. 10 Natural gas supply of the SOFC

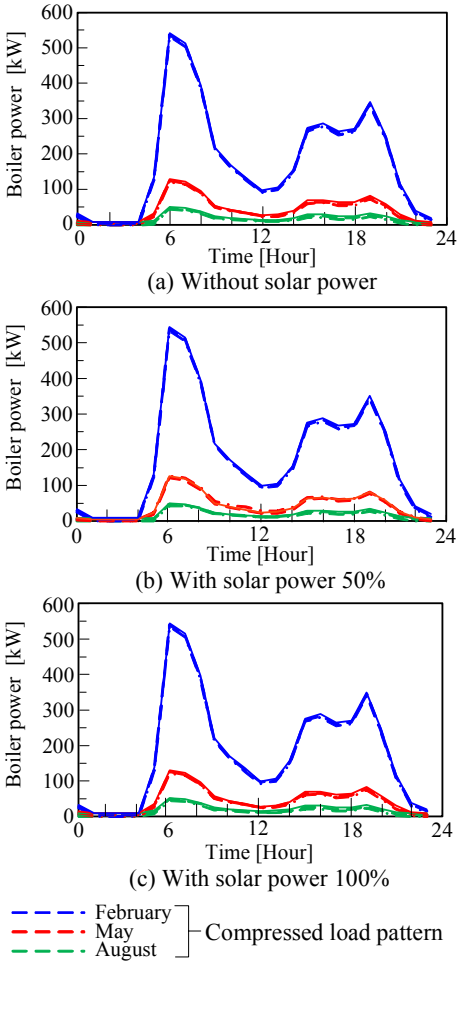

Fig. 11 Boiler power supply of the SOFC

(average, compressed and extended load patterns) and at 0% (without solar power), 50% and 100% output solar power. The amount of photovoltaic power generated is calculated using the NWI and Eq. (1) to (5). In this analysis, the average value in Sapporo in 1990 to 2003 is used as the NWI. The production of electricity at this time is set to 100%. In consideration of a cloudy sky etc., the case of solar power at 50% and 0% (without solar power) is also analyzed. In the analysis of this paper, 30 kW photovoltaic power generation (145 W/m^2, efficiency of the power generation is 14%) is introduced. The load factor of each fuel cell in daytime falls by this photovoltaic power generation.

The operation plan of only the SOFC to supply the demand side is shown in Figs. 9 to 11. Moreover, the operation plan of only the PEFC to supply the demand side is shown in Figs. 12 to 14. As shown in Figs. 9 and 12, the power generation efficiency of the SOFC independent operation is large compared with the PEFC independent operation. When the amount of photovoltaic power generated increases, the load of the fuel cell falls. As a result, the power generation efficiency of the fuel cell falls. The analysis results for the fuel consumption of the SOFC and PEFC are shown in Figs. 10 and 13. When the amount of photovoltaic power generated is large, the fuel consumption of the fuel cell increases because the partial-load operation with low fuel cell efficiency occurs. On the other hand, because the amount of solar radiation fluctuates greatly, the amount of photovoltaic power generated changes. Therefore, as shown in Figs. 10 and 13, the fuel consumption of the fuel cell in the daytime has sharp changes.

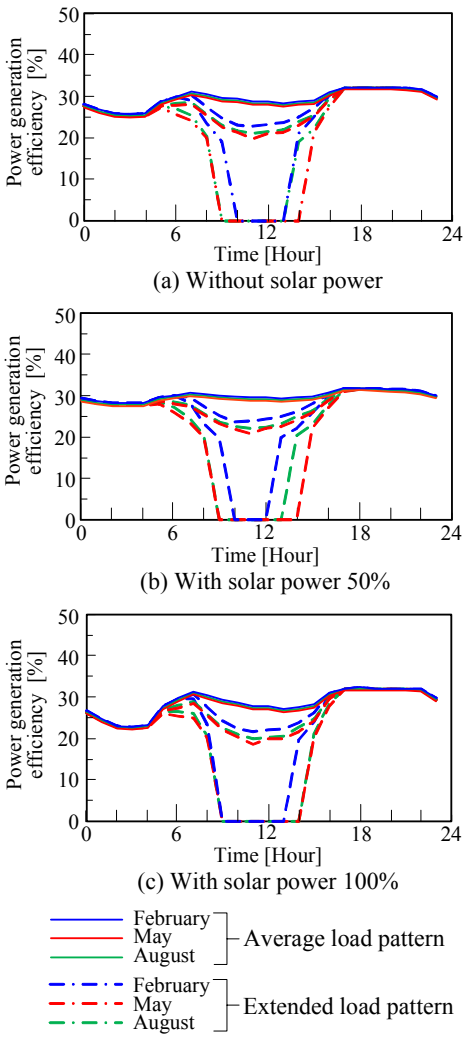

Fig. 12 Power generation efficiency of the PEFC

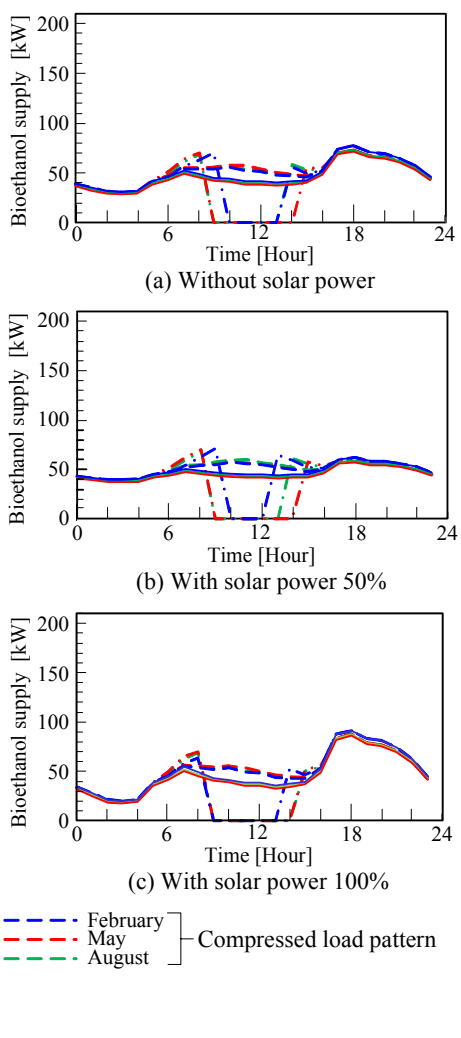

Fig. 13 Bioethanol fuel supply of the PEFC

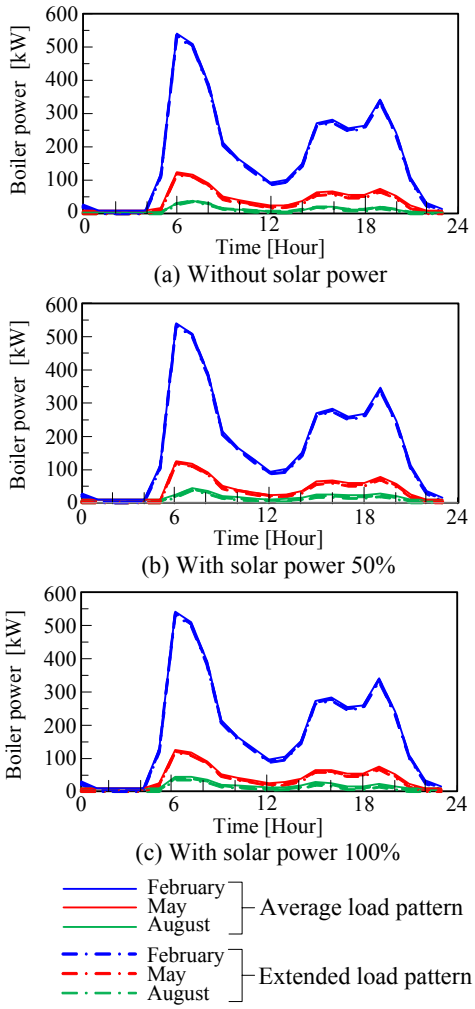

Fig. 14 Boiler power supply of the PEFC

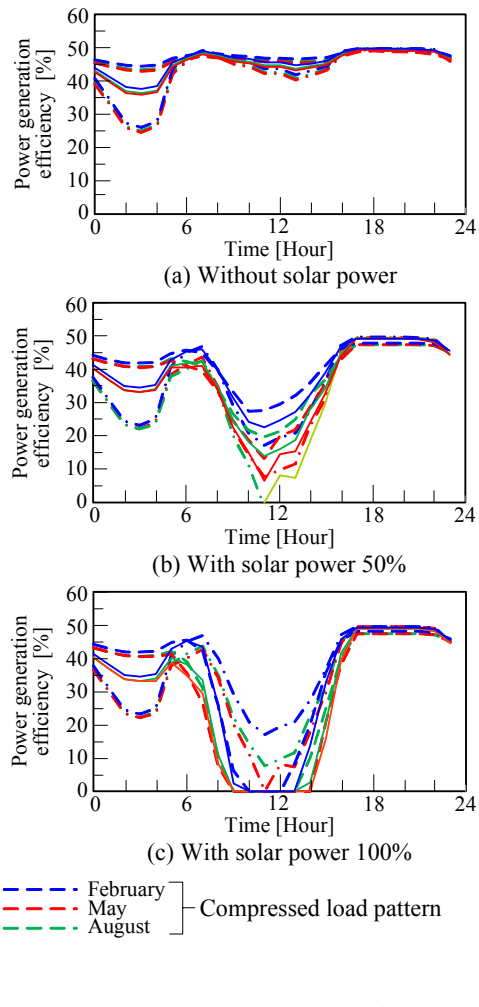

Fig. 15 Power generation efficiency of the SOFC-PEFC combined system

Figures 11 and 14 show the analysis results of the boiler operation of the SOFC and PEFC independent systems, respectively. Because the heat load is very large compared with the power load, the difference between the SOFC independent system and the PEFC independent system is small.

The operation plan of the SOFC-PEFC combined system is shown in Figs. 15 to 18. Figure 15 shows the analysis results of the power generation efficiency of the proposed system. When photovoltaic power generation is not introduced (Fig. 15 (a)), the change in the power generation efficiency is small. However, the load factor of the system falls when the amount of photovoltaic power generated increases. Therefore, the proposed system differs in performance according to the season and the weather.

Figures 16 and 17 show the analysis results for the consumption of the bioethanol supplied to the reformer (R/M) and the natural gas supplied to the SOFC, respectively. From the consumption of natural gas shown in Fig. 17, the power load peak at 16:00 to 22:00 shown in Fig. 7 (a) is leveled by the operation of the SOFC. On the other hand, if the amount of photovoltaic power generated increases, the amount of daily bioethanol supplied to the reformer (R/M) will increase, as shown in Fig. 16. Because the load factor of the SOFC will fall if the power supply from photovoltaic power generation increases, the power generation efficiency falls. Therefore, because the amount of exhaust heat from the SOFC increases, the amount of bioethanol supplied to the reformer increases. Figure 18 shows the analysis results of the boiler operation. These results are the same as the results of Figs. 11

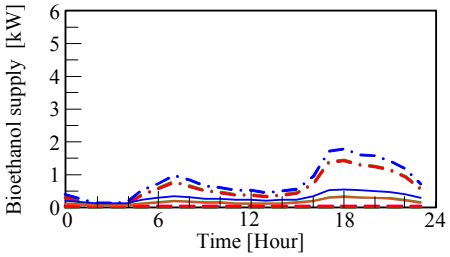

(a) Without solar power

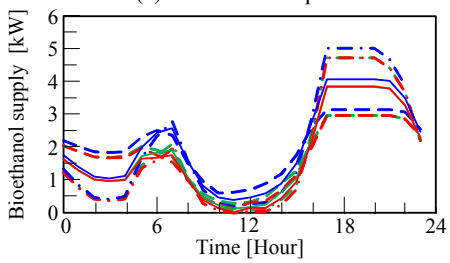

(b) With solar power 50%

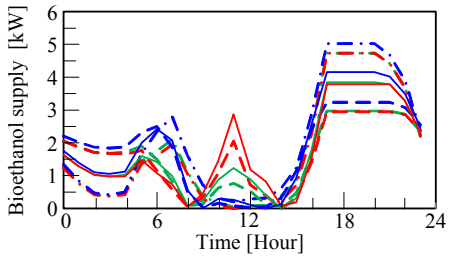

(c) With solar power 100%

Fig. 16 Bio-ethanol supply of the SOFC-PEFC combined system

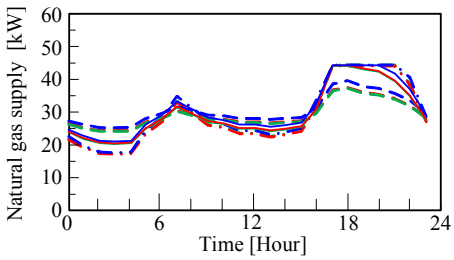

(a) Without solar power

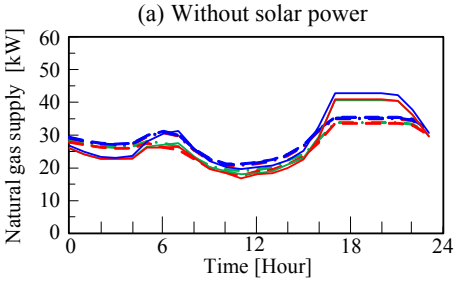

(b) With solar power 50%

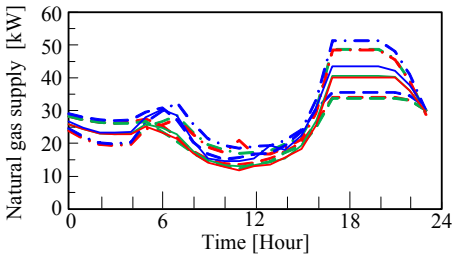

(c) With solar power 100%

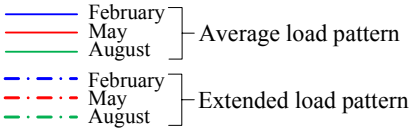

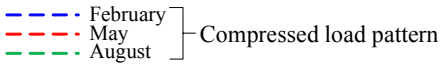

Fig. 17 Natural gas supply of the SOFC-PEFC combined system

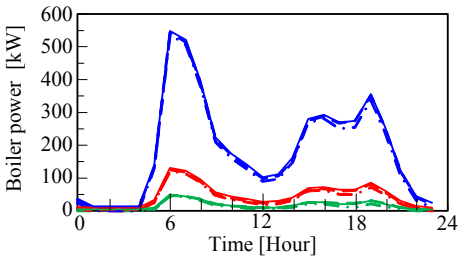

(a) Without solar power

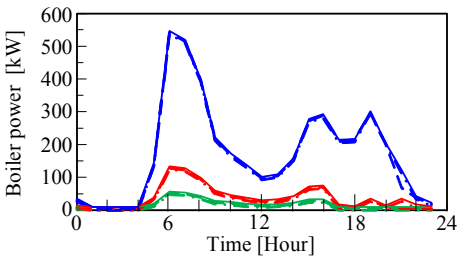

(b) With solar power 50%

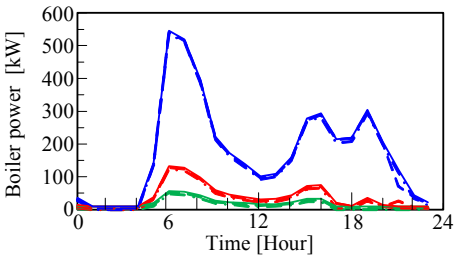

(c) With solar power 100%

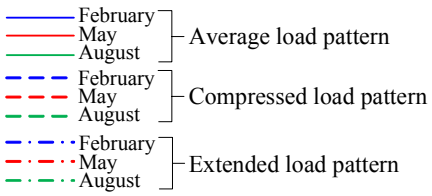

Fig. 18 Boiler power supply of the SOFC-PEFC combined system

and 14. Because the heat load (Fig. 7 (b)) used in this analysis is large compared with the system exhaust heat (reformer (R/M), the condenser unit (C/U) and the PEFC in Fig. 1 (b)), the difference in the boiler operation between each system is small.

Figure 19 shows the heat storage quantities in case of average load patterns of a

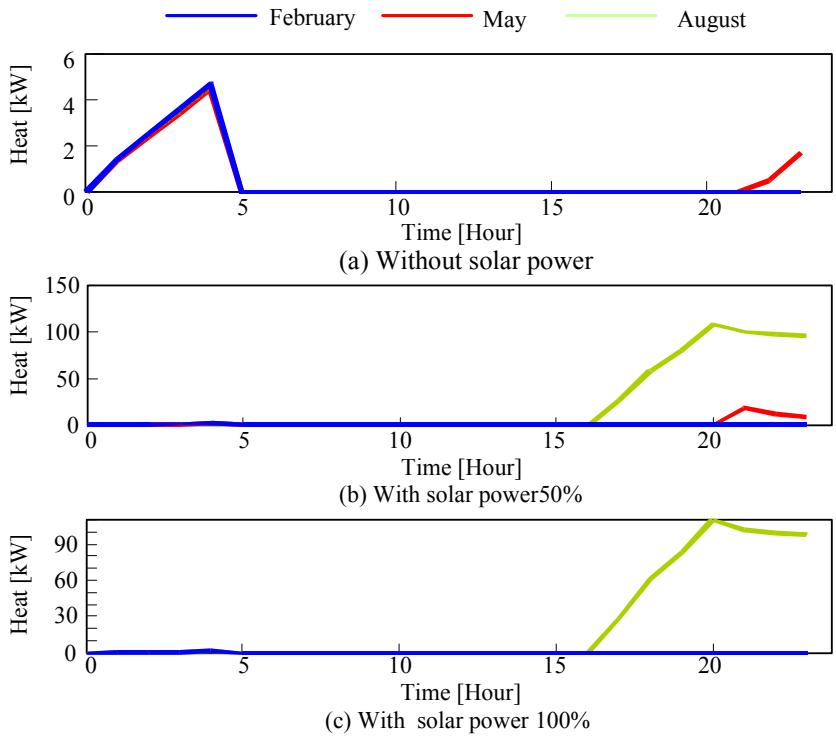

Fig. 19 Heat storage quantities in case of average load patternof the SOFC-PEFC combined system

representative day in each month. As shown in this figure, the hightest values of heat storage occurs in August due to the smallest heat demand in this month compared to the other two months.

Figure 20 shows the analysis results for the fuel consumption in each system of a representative day every month. In the SOFC, the PEFC and the SOFC-PEFC combined system, natural gas, bioethanol, natural gas and bioethanol are consumed. Figure 20 (a) shows the results, not including boiler fuel. On the other hand, Fig. 20 (b) shows the results including boiler fuel. In Fig. 20 (a), the fuel consumption of the SOFC-PEFC combined system is reduced 10 to 35% compared with the SOFC or PEFC independent system. If boiler fuel is added to the fuel consumption of the fuel cell, as shown in Fig. 20 (b), the fuel consumption in May and August will decrease greatly. Because the heat load of the winter season in a cold, snowy area is very large compared with the power load, there are few reduction effects of the fuel consumption of the proposed system with boiler fuel.

On the other hand, because there is little heat load in mid-term and the summer season, the effect of the fuel reduction of the proposed system is large.

Figure 21 shows the daily mean power generation efficiency of the SOFC-PEFC combined system. The power generation efficiency considering all load patterns of the proposed system is 27% to 48%. Although the power generation efficiency changes according to the season and load pattern, the photovoltaic power influences the system efficiency most strongly. When introducing photovoltaic power into an independent microgrid, the improvement of the efficiency decrease due to the partial-load operation of the fuel cells is important.

6. Conclusions

The SOFC-PEFC combined system with a time shitting of reformed gas is proposed to supply energy to a micro-grid consisting of 30 residences in Sapporo, Japan. Three cases are

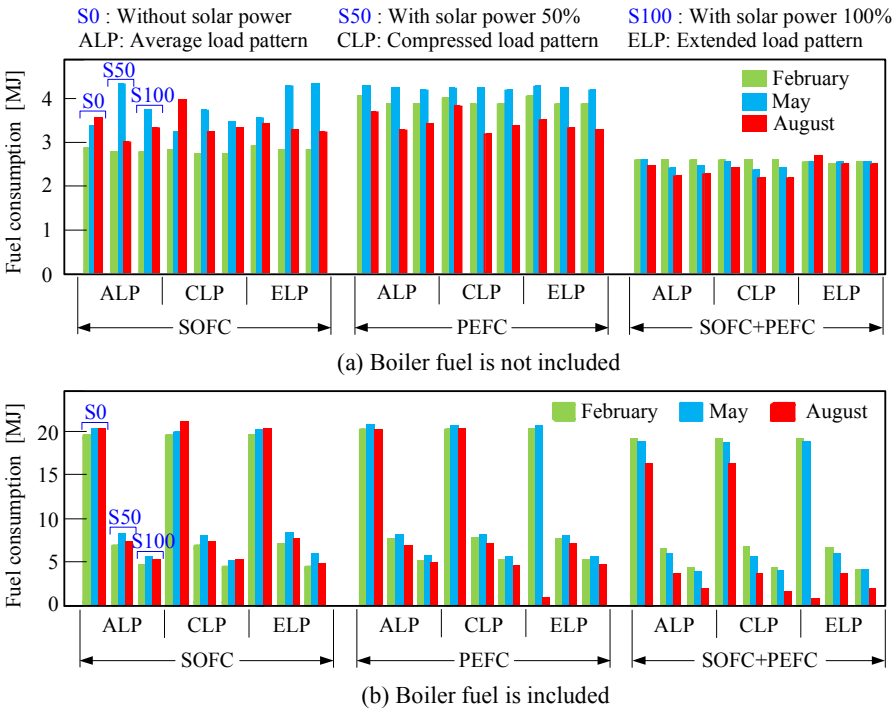

(a) Boiler fuel is not included

(b) Boiler fuel is included

Fig. 19 Analysis result of the fuel consumption of a representative day

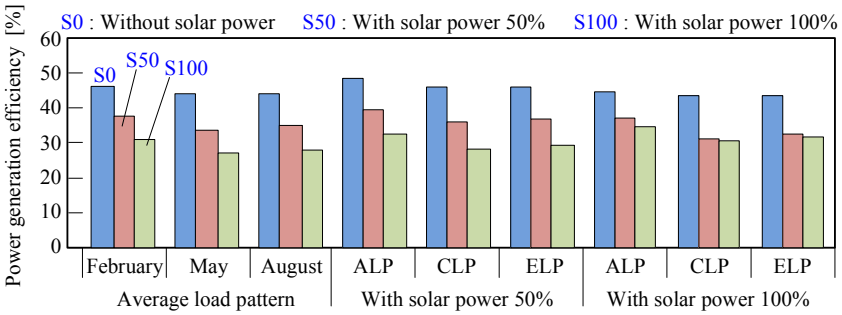

Fig. 20 Total power generation efficiency on a representative day of the SOFC-PEFC combined system

proposed for the operation plan of the SOFC-PEFC combined system without a PV system and with 50% and 100% solar power. The following conclusions are obtained:

(1) When photovoltaic generation is not introduced into the SOFC-PEFC combined system, the change in the power generation efficiency is small. However, the load factor of the proposal system falls when the amount of photovoltaic power increases.

(2) On the other hand, if the amount of photovoltaics power generated increases, the amount of daily bioethanol supplied to the reformer will increase. Because the load factor of the SOFC decreases if the power supply due to photovoltaic power increases, power generation efficiency decreases. Therefore, because the amount of exhaust heat from the SOFC increases, the amount of bioethanol supplied to the reformer increases. In other words, the proposed system differs in performance according to the season and the weather.

(3) The fuel consumption of the SOFC-PEFC combined system is reduced 10 to 35% compared with the SOFC or PEFC systems independently. If boiler fuel is added to the fuel consumption of the fuel cell, the fuel consumption in May and August will decrease greatly. Because the heat load of the winter season in a cold, snowy area is very large compared with the power load, there are few reduction effects on the fuel consumption of the proposed system.

(4) The power generation efficiency considering three load patterns (average load pattern,

compressed load pattern and extended load pattern) of the proposed system is 27% to 48%. However, because the heat load is very large compared with the power load, the difference between the SOFC independent system and the PEFC independent system is small.

Acknowledgments

This work was partially supported by a Grant-in-Aid for Scientific Research (C) from JSPS.KAKENHI (20560204).

References

(1) Naim H. Afgan, Maria G. Carvalho, Sustainability assessment of hydrogen energy systems, International Journal of Hydrogen Energy, Vol. 29, No. 13, (2004), 1327-1342.

(2) Muhsin Tunay Gencoglu, Zehra Ural, Design of a PEM fuel cell system for residential application, International Journal of Hydrogen Energy, Vol. 34, No. 12, (2009), 5242-5248.

(3) Georg Erdmann, Future economics of the fuel cell housing market, International Journal of Hydrogen Energy, Vol. 28, No. 7, (2003), 685-694.

(4) Tak-Hyoung Lim, Rak-Hyun Song, Dong-Ryul Shin, Jung-Il Yang, Heon Jung, I.C. Vinke, Soo-Seok Yang, Operating characteristics of a 5 kW class anode-supported planar SOFC stack for a fuel cell/gas turbine hybrid system, International Journal of Hydrogen Energy, Vol. 33, No. 3, (2008), 1076-1083.

(5) S. H. Chan, H. K. Ho, Y. Tian, Multi-level modeling of SOFC–gas turbine hybrid system, International Journal of Hydrogen Energy, Vol. 28, No. 8, (2003), 889-900.

(6) Ali Volkan Akkaya, Bahri Sahin, Hasan Huseyin Erdem, An analysis of SOFC/GT CHP system based on exergetic performance criteria, International Journal of Hydrogen Energy, Vol. 33, No. 10, (2008), 2566-2577.

(7) Sadegh Motahar, Ali Akbar Alemrajabi, Exergy based performance analysis of a solid oxide fuel cell and steam injected gas turbine hybrid power system, International Journal of Hydrogen Energy, Vol. 34, No. 5, (2009), 2396-2407.

(8) Y. Haseli, I. Dincer, G.F. Naterer, Thermodynamic modeling of a gas turbine cycle combined with a solid oxide fuel cell, International Journal of Hydrogen Energy, Vol. 33, No. 20, (2008), 5811-5822.

(9) Fumihiko Yoshiba, Yoshiyuki Izaki, Takao Watanabe, Wide range load controllable MCFC cycle with pressure swing operation, Journal of Power Sources, Vol. 137, (2004), 196–205.

(10) Online data service, GPV/GSM (Grid Point Value / GSM (Global Spectral Model)), http://www.jmbsc.or.jp/hp/online/f-online0a.html, Japan meteorological business support center, (2009).

(11) Data of Japan Meteorological Agency, http://database.rish.kyoto-u.ac.jp/arch/jmadata/gpv-original.html, Kyoto University, (2009).

(12) Yasuda I., Development of Hydrogen Production Technology for Fuel Cell, Energy Synthesis Engineering, Vol. 28, No.2, (2005).

(13) T. Nakamura and M. Sei., Energy Related Technology. High-Efficiency Fuel Processor for Fuel Cell System, Technical Report, Vol. 77, (2002), 4-9, Matsushita Electric Works, Ltd.

(14) K. Oda, A Small-scale Reformer for Fuel Cell Application, Sanyo technical review, Vol. 31, No.2, (1999), 99-106.

(15) Shin'ya Obara: “Power Generation Efficiency of an SOFC-PEFC combined System with

time shift Utilization of SOFC exhaust heat“, International Journal of Hydrogen Energy, Vol. 35, No. (2), (2010), 757-767.

(16) Shin'ya Obara and Abeer Galal El-Sayed: “Compound Microgrid Installation Operation Planning of PEFC and Photovoltaics with Prediction of Electricity Production using GA and Numerical Weather Information“, International Journal of Hydrogen Energy, Vol. 34, No. (19), (2009), 8213-8222.

(17) Solar Energy Utilization Handbook, Japan Solar Energy Society, Ohmsha, Ltd, (1985), 10-88.

(18) NEDO Technical information database, Standard meteorology and Solar radiation data (METPV-3), http://www.nedo.co.jp.

(19) Daisuke Okawa, Naoki Shikazono and Nobuhide Kasagi: “Basic Characteristics of Gas Turbine-Solid Oxide Fuel Cell Hybrid System with Air Reduction”, Transactions of the JSME, Series B, 73(730), (2007), 113-120.(in Japanese).

(20) Development of a several 10kW class circular-flat-type low-temperature operation SOFC system, Result report symposium 2007, New Energy and Industrial Technology Development Organization in Japan, http://www.nedo.go.jp/informations/events/200623/26_7.pdf, (in Japanese)

(21) Takeda, Y. et al., Development of Fuel Processor for Rapid Start-up, Proc. 20th Energy System Economic and Environment Conference, Tokyo, January 29-30, ed., K. Kimura, (2004), 343-344.

(22) Mikkola, M., Experimental Studies on Polymer Electrolyte Membrane Fuel Cell Stacks, Master's thesis submitted in partial fulfillment of the requirements for the degree of Master of Science in Technology, Helsinki University of Technology, (2001), 58-79.

(23) Shin'ya Obara: “Improvement of Power Generation Efficiency of an Independent Micro Grid Composed of Distributed Engine Generators”, ASME Trans. Journal of Energy Resources Technology, Vol. 129, Issue 3, (2007), 190-199.

(24) Narita k. Research on unused energy of cold region cities and utilization for district heat and cooling. Ph.D thesis, Dep. Socio-Environmental Eng. Faculty of Eng., Hokkaido Univ. Sapporo, Japan, 1996.